Cone Penetration Testing 2018 – Hicks, Pisanò & Peuchen (Eds)

Numerical simulation of cone penetration test in a small-volume calibration chamber: The effect of boundary conditions

M. Goodarzi
MARUM—Center for Marine Environmental Sciences, University of Bremen, Bremen, Germany
Geo-Engineering.org GmbH, Bremen, Germany

F.T. Stähler & S. Kreiter
MARUM—Center for Marine Environmental Sciences, University of Bremen, Bremen, Germany

M. Rouainia
School of Engineering, Newcastle University, Newcastle upon Tyne, UK

M.O. Kluger
MARUM—Center for Marine Environmental Sciences, University of Bremen, Bremen, Germany

T. Mörz
MARUM—Center for Marine Environmental Sciences, University of Bremen, Bremen, Germany
Geo-Engineering.org GmbH, Bremen, Germany

ABSTRACT: In this study, laboratory Cone Penetration Tests (CPTs) were conducted in the MARUM Calibration Chamber (MARCC) with three lateral boundary conditions: (BC), constant stress, constant strain and the simulated field conditions with constant stiffness. Cuxhaven-Sand was studied in the chamber tests and tip resistance-relative density ($q_c - D_r$) relationships were generated for each BC. Laboratory experiments were carried out to estimate the mechanical properties of the Cuxhaven-Sand. Multiple numerical analysis have then been undertaken to simulate the calibration chamber results. First, the soil model was calibrated against laboratory soil parameters and a CPT result of the calibration chamber with fixed lateral boundaries, then, a numerical penetration analysis in an infinite soil mass was performed to evaluate the implemented constant stiffness boundary condition in the chamber. Good agreement between experimental and numerical cone resistances demonstrates the possibility of using the advanced small volume MARCC for producing controlled CPT results applicable in true field test conditions.

1 INTRODUCTION

Calibration chambers (CCs) play a crucial role in the interpretation and analysis of cone penetration test (CPT) results. The advantage of cone penetration tests in a CC is that material properties and the stress state of the sample can be controlled. Therefore, uncertainties in the dependency of cone resistances on soil and stress state are less ambivalent than in field tests. The conventional boundary conditions of the sample in a CC are either constant stress or constant strain in lateral and vertical directions. Two widely used boundary conditions are BC1 and BC3. In both cases the vertical stress boundary is applied, the lateral boundary in BC1 applies a constant stress, while in BC3 the lateral displacement is fully constrained, which results in a constant strain (Salgado et al., 2001). Despite the advantages of CC tests, the limited size of the sample or chamber may impose boundary effects on the measured cone resistance. This phenomenon was observed when different chambers or cone sizes were adopted for tests under BC1 and BC3 along with defined materials or stress conditions (Jamiolkowski et al., 1985). Moreover, the boundary effect may also be related to the soil density. For example, Schnaid & Houlsby (1991) reported an increase of boundary effect with increase in relative density (D_r) under BC1 conditions.

The calibration of field CPT data with laboratory CC experiments requires either the sample to be large enough or the measured q_c to be corrected for boundary effects. Parkin and Lunne (1982) concluded that the boundary effect is negligible when the ratio of sample to cone diameter (R_d) is larger than 50 and Jamiolkowski et al. (2003)

recommended a R_d of at least 70. Working with such big CC is technically and economically more challenging regarding the amount of materials needed and the time spent on sample preparation. Therefore, some studies attempted to establish correction factors for the q_c values measured in small volume CC by comparing the values of CC with field tests (Mayne & Kulhawy, 1991; Jamiolkowski et al., 1985; 2003; Butlanska et al., 2009). A problem associated with these studies is that the correction factors are determined for specific samples, cone sizes or sands. Therefore, they cannot be generally used for all CC test. Another approach to tackle the size effect is to impose a constant stiffness on the lateral boundary of the sample and to simulate an infinite soil mass. Huang & Hsu (2005), following the work of Ladanyi (1972), proposed a stress-strain relation for the lateral stiffness boundary utilizing the equilibrium equation in cylindrical coordinates. The stress-strain response of the soil is first determined by compressing the sample in the lateral direction and then the obtained radial stress-strain relationship is used to replicate the stress on a sample embedded in an infinite soil mass. This boundary condition is called BC5 or simulated field boundary condition. Their sample in CC is confined with several rings and each ring controls the required stress strain relationship independently.

In this study, a small volume CC (Fleischer et al., 2016) with a R_d of 25 was equipped with three circumferential strain sensors. The approach initially proposed by Ladanyi (1972), which has the aim to determine the undrained shear strength of clay using a pressuremeter, was reformulated for CC in order to estimate the imposed stress at the sample boundary under BC5. An important step is to validate this new boundary condition and to prove that the stress state inside the chamber is comparable to the stress of an infinite soil mass. For this purpose, several chamber tests were conducted under BC1, BC3 and BC5 and the q_c-D_r relationships were generated for these boundary conditions. Cuxhaven-Sand, an onshore material analogous to Pleistocene Southern North Sea sand was used as the sample material. Then, numerical models of the chamber with these three boundary conditions were generated using the commercial finite element (FE) software ABAQUS (Abaqus manual version 6.11). Mohr-Coulomb soil parameters were obtained from triaxial testing and then the soil model was calibrated using CC test with the constant strain boundary condition of BC3. The numerical results were compared with the CC tests under both BC1 and BC5 in order to evaluate the capability of the CC in reproducing q_c, comparable with CPT tests in an infinite soil mass.

2 THE SMALL VOLUME CALIBRATION CHAMBER

2.1 *Overview*

A small volume CC was developed in Marine Engineering Geology working group of the Center for Marine Environmental Sciences (MARUM), University of Bremen (Fleischer et al., 2016). The MARUM CC (MARCC) is similar to a large triaxial cell with a sample of 300 mm in diameter and 550 mm in height placed in a latex membrane (Fig. 1). An in-house designed small cone with a 12 mm diameter is used for the tests resulting in a R_d of 25. The chamber is equipped with three LVDT circumferential sensors to measure the lateral strain of the sample throughout the tests. The LVDT sensors are placed at vertical distances of 150, 250 and 350 mm from the top of the sample.

2.2 *Boundary conditions*

MARCC has different vertical and lateral boundaries. The top boundary of the sample is a fixed sintered steel plate, while the lower boundary is a stress-controlled water filled cushion and applies a constant pressure. The lateral boundary can be fully fixed by using a rigid steel casing, which is used for boundary condition BC3 (Fig. 2). The BC1 is realized by regulating constant pressure around the latex membrane of the sample in CC.

The complexity, however, lies in the implementation of the simulated field boundary condition BC5 in the MARCC. In an ideal scenario, the BC5 should reproduce the stress and strain at the sample lateral boundary in such a way that the sample is embedded in an infinite soil mass (Fig. 3).

While BC1 and BC3 are independent of soil properties and the sample size, BC5 simulates the material dependent displacement and induced

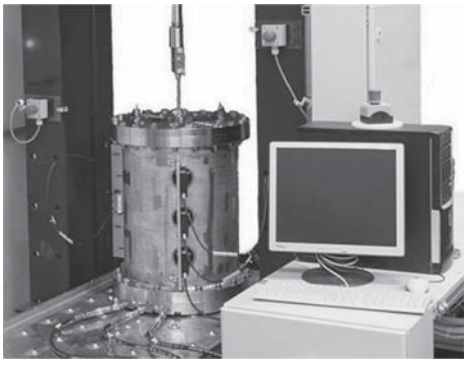

Figure 1. An overview of the calibration chamber facility MARCC at MARUM, University of Bremen.

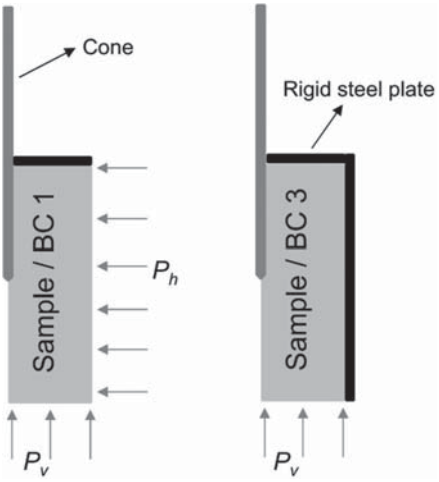

Figure 2. Axisymmetric schematic drawing of the BC1 and BC3 in the CC.

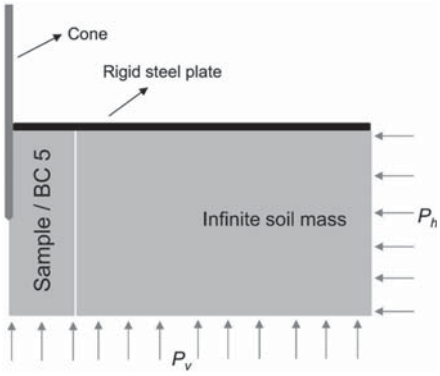

Figure 3. Axisymmetric schematic drawing of an ideal BC5 in the CC.

stress at the lateral boundary. The actual lateral stress in BC5 thus depends on how the soil deforms during penetration. In order to derive an analytical expression for the stress-strain response around a cylindrical cavity expansion, Ladanyi (1972) proposed to use the equilibrium equation in cylindrical coordinates with no body forces and no vertical stress variation as follows:

$$\frac{d\sigma_r}{dr} + \frac{\sigma_r - \sigma_\theta}{r} = 0 \tag{1}$$

where r is the radius and σ_r and σ_θ are the total principle stresses in radial and tangential directions, respectively. As the σ_r and σ_θ are the principal stresses, the term σ_r - σ_θ is a deviatoric stress, q.

The equilibrium equation should be satisfied at any point inside the sample and on the boundary. During penetration the cavity radius expands, Equation 1 is then integrated for any incremental change in the sample radius for r_i to r_{i+1} as follows:

$$\int_i^{i+1} d\sigma_r = \int_i^{i+1} \frac{q_{i,i+1}}{r} dr \tag{2}$$

where $q_{i,i+1}$ is the deviatoric stress at increment i to $i+1$. Assuming a constant $q_{i,i+1}$ through each incremental radius change. After some mathematical calculation, Equation 2 can be rewritten as:

$$\sigma_r^{i+1} = -q_{i,i+1}(\ln(1+\varepsilon_r^{i+1}) - \ln(1+\varepsilon_r^{i})) + \sigma_r^{i} \tag{3}$$

where ε_r is the radial strain and the superscript i is the increment number.

Equation 3 is an analytical expression of radial stress and radial strain around the axis of symmetry of the sample. The term $q_{i,i+1}$ is a function of the stress level, the distance from the center of cavity expansion and the soil mechanical response. If it is assumed that the elastic response of the soil under small deformation at the chamber boundary is similar in both compression and expansion, $q_{i,i+1}$ can be evaluated by an initial lateral compression of the sample. Therefore, after the preparation and consolidation of the sample, the lateral stress is incrementally increased by 10 kPa/min until a maximum radial strain of 0.08% is reached. The radial strain is derived from the circumferential LVDTs and allows a relationship between $q_{i,i+1}$ and ε_r to be established.

When the cone penetrates under BC5, the required incremental increase in the lateral stress is calculated for each increment of radial strain and its corresponding $q_{i,i+1}$ using Equation 3.

Within the MARCC, the increase in lateral stress is controlled by the maximum radial strain recorded with the three LVDTs. This potentially introduces some artefacts, as the stress increases around the whole height of the chamber uniformly and the radial strain measurement is only at three levels. The effectiveness of this approach for incorporating simulated field boundary condition in calibration chambers is discussed in Section 6.

3 MECHANICAL PROPERTIES OF CUXHAVEN SAND

The mechanical properties of the Cuxhaven-Sand are needed to perform numerical analysis of the CPTs in MARCC. A linear elastic-perfectly plastic behaviour with Mohr-Coulomb failure envelope was chosen for this study, requiring the elastic parameters, the internal friction angle and dilation angle of Cuxhaven-Sand.

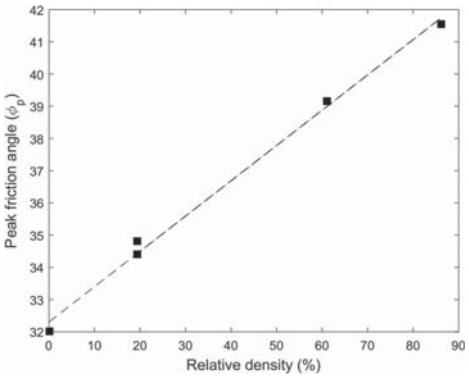

Figure 4. Peak friction angle as a function of relative density.

A correlation between the peak/critical friction angle and relative density for Cuxhaven sand was derived by a sequence of monotonic triaxial compression tests and sand cone pluviation tests, following procedures outlined in Wichtmann (2005) (Fig. 4). The critical friction angle is 32 degree and the dilation angle is estimated using

$$\psi = \varphi'_P - \varphi'_C \,, \tag{4}$$

where φ'_p and φ'_c are the peak and critical friction angles and ψ is the dilation angle (Susila and Hryciw, 2003).

The Young's modulus, of the soil significantly controls the concentration of induced stress around the cone. The Young's modulus is nonlinear and known to be affected by the mean effective stress (Susila & Hryciw, 2003; Tolooiyan & Gavin, 2011). Therefore, CPT results are used to calibrate this parameter for the Cuxhaven-Sand.

In order to estimate the relative density of the Cuxhaven-Sand inside the chamber, the maximum and minimum void ratio was determined following DIN 18126 (1996) and the relative density is calculated as:

$$D_R = \frac{e_{\max} - e}{e_{\max} - e_{\min}} = \frac{0.82 - e}{0.82 - 0.48} \tag{5}$$

where e_{max}, e_{min} and e are the maximum, minimum and actual void ratio, respectively.

4 CPT IN MARCC WITH DIFFERENT BOUNDARY CONDITIONS

The q_c-D_r relationships of the Cuxhaven-Sand for BC1, BC3, and BC5 conditions were established for initial relative densities ranging from dense to very dense based on several tests per boundary condition (Fig. 5).

All samples were prepared by air pluviation to relative densities between $D_R = 0.75$ and $D_R = 0.95$. Air-pluviated samples were vacuum saturated in MARCC by allowing de-aired and demineralized water to slowly percolate from the bottom to the top of the sample. A Skempton B-value of at least 0.95 was reached for all tests. Vertical and radial consolidation stresses of 300 kPa and 190 kPa were applied, respectively and a back pressure of 100 kPa was realized. These conditions represent a burial depth of around 18 m to 20 m, which is important for offshore wind turbine foundations. All saturated and consolidated samples were penetrated by a 12 mm cone under drained conditions with a constant penetration speed of 2 cm/s.

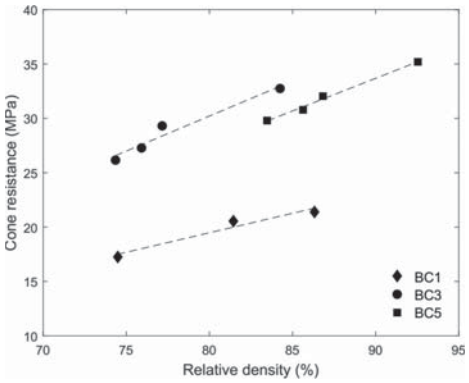

Figure 5. CPT results in Cuxhaven sand obtained in MARCC with different boundary conditions.

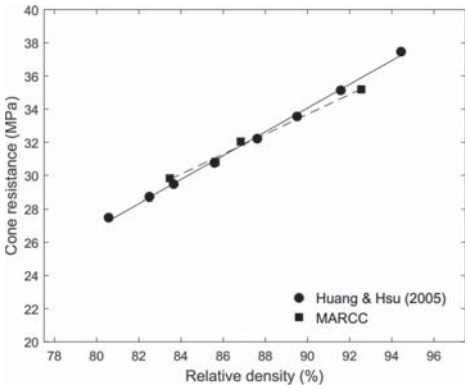

Figure 6. Comparison between CPT results obtained in Huang & Hsu's (2005) chamber and MARCC under BC5.

Figure 5 provides the $q_c - D_r$ relationships obtained with different boundary conditions. One data-point for CPT represents the steady-state cone resistance over a penetration depth of usually 150–300 mm. As expected, the constant stress boundary condition BC1 results in the lowest q_c values and the constant strain boundary condition BC3 gives the highest. The simulated field boundary condition, BC5 shows values between BC1 and BC3.

The larger CC of Huang & Hsu (2005) with its independent circumferential rings is, despite our use of only one lateral stress and the use of a different sand, in good agreement with the results presented in this study (Fig. 6).

5 NUMERICAL MODELLING OF CALIBRATION CHAMBER TESTS

The numerical analyses of the CC tests were carried out using the commercial finite element package, ABAQUS (Abaqus manual version 6.11). The symmetry around the cone axis allows an axisymmetric formulation for the model set up. Suitable mesh refinement around the cone is an important numerical parameter, which needs to be determined in order to avoid mesh-dependency in the results. As there is no rule of thumb, the appropriate mesh size is evaluated by repeated runs with a stepwise mesh refinement until the value of q_c stays constant.

The penetration process of CPT involves large deformation of the soil around the cone. Therefore, the arbitrary Lagrangian-Eulerian (ALE) formulation, implemented in ABAQUS, is used as a means to avoid the excessive mesh distortion around the cone, which could terminate the solution. This method allows for the adjustment of the aspect ratio of elements around the cone where excessive deformation takes place (see Hu &Randolph, 1998). The ALE formulation is only applied to a zone round the penetration path.

The soil mass is considered to be weightless and elastic-plastic using the Mohr-Coulomb failure criteria. The solution is explicit dynamic so axisymmetric linear elements (CAX4R) are used. The cone and rod is assumed to be rigid, therefore an analytical rigid surface is adopted to represent them. As the tests are static CPT in highly permeable sand, it is assumed that the system is drained. Therefore, based on the values of pore pressure and total stresses mentioned in Section 4, the numerical analyses are conducted with the effective stresses of 200 kPa and 90 kPa for vertical and lateral boundaries, respectively. The contact friction between the cone and the sand is assumed half of the internal friction angle of the soil (Susila & Hryciw, 2003).

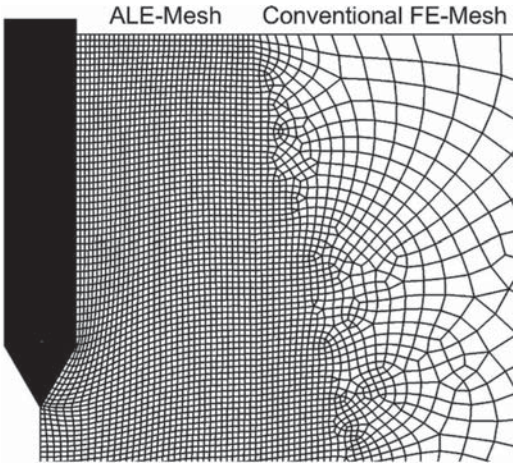

Figure 7. Deformed mesh around the cone in the FE model.

The BC1 and BC3 boundary conditions are applied as constant stress or fixity at the boundaries. However, in order to test the BC5 of the MARCC in the numerical model, an infinite soil mass is required in the lateral direction of the chamber. Therefore, the lateral boundary is extended (see Figure 3) four times leading to $R_d = 125$, which is beyond the recommended value of 70 for CC. The employed mesh refinement around the cone and the quality of the deformed mesh with ALE formulation is presented in Figure 7.

6 NUMERICAL ANALYSES OF CPTS IN MARCC

6.1 *Calibration of the stiffness of Cuxhaven-Sand with CPT results*

BC3 is the best-defined boundary condition consisting of a top and circumferential fixity with only the lower boundary being subjected by variable but constant stresses. Therefore, BC3 tests were selected for the purpose of model calibration using the soil stiffness for the Cuxhaven-Sand as a variable. A relative density was chosen for the calibration and its corresponding mechanical properties are derived from experimental results, whereas the Poisson's ratio (υ) is assumed (Table 1).

Several attempts with different elastic modulus values were conducted in order to calibrate this parameter for a relative density of 82% and the best result is presented in Figure 8 along with two other trials. An E of 50 MPa results in a cone resistance of almost 31 MPa, which is similar to the measured cone resistance in the CC test. It is also observed that the Young's modulus of the

Table 1. Experimental data for the selected relative density.

Parameters	Values
Relative density (D_r)	82%
Peak friction angle (φ'_p)	41
Critical friction angle (φ'_c)	32
Dilation angle (ψ)	9
Young's modulus (E')	?
Poisson's ratio (υ)	0.3
Cone resistance, q_c (MPa), in MARCC with:	
BC1	20.2
BC3	31
BC5	29

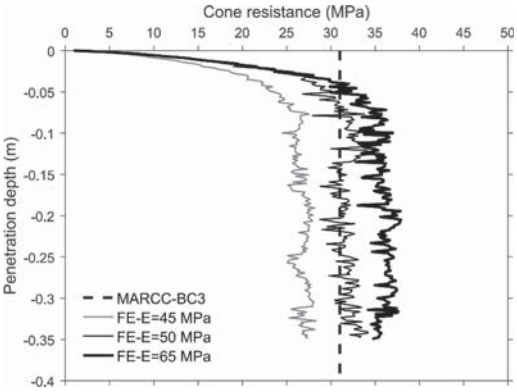

Figure 8. Three trial numerical CPT curves for CC test under BC3 with soil parameters presented in Table 1 and different Young's moduli, the straight-line represents the average value of the steady state part of the experimental CPT curve.

Cuxhaven-Sand has a significant effect on the simulated q_c due to its influence on the induced stress concentration around the cone.

The value of 50 MPa for this sand for a mean effective stress (p') of 126.7 kPa is in good agreement with the experimental graph of p'-E reported by Tolooiyan & Gavin (2011) for Blessington Sand, which gives $E = 50.6$ MPa for the same p'.

6.2 *Prediction of the CPT results in MARCC under BC1 and BC5*

The set of mechanical properties of Cuxhaven-Sand with relative density 82%, achieved in the previous section, is used in order to predict the cone resistance in CC with BC1 and BC5. Comparing the numerical result with the CC test is important in two aspects. First, it is interesting to see how well the boundary effects are reproduced in FE analyses. This could potentially help to determine boundary

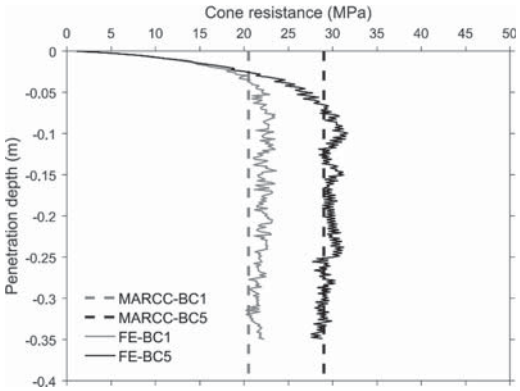

Figure 9. Numerical and experimental results for the uncalibrated CPTs in CC under BC1 and BC5. The straight-lines represent the average values of the steady state part of the experimental CPT curves.

effect correction factors for the CC results using finite element analysis. Second, as the numerical CPT with BC5 has an actual infinite lateral boundary, it allows us to evaluate the performance of the implemented BC5 in MARCC.

Figure 9 shows the numerical CPT curve versus the q_c measured in MARCC with both uncalibrated boundary conditions BC1 and BC5. A good agreement between FE analyses and the experimental results is observed. It can be concluded that the less sophisticated set-up in MARCC for the simulated field boundary is effective enough to produce CC's results, which are comparable to CPTs in infinite soil mass. A slight error in reproducing CPT results under BC1 condition can be seen. This issue could potentially be due to the simplicity of the soil model or caused by friction on the lateral boundary in the MARCC test, which was considered as frictionless in the numerical model.

7 CONCLUSION

In this study, the small volume calibration chamber MARCC was equipped with circumferential strain gauges and a servo-control lateral pressure system in order to reproduce the so-called simulated field boundary conditions BC5. This boundary condition allows production of CPT results comparable to field tests in calibration chambers. A numerical analysis was then used to evaluate the performance of the implemented boundary conditions.

Through several numerical and experimental CPTs with Cuxhaven-Sand, it was shown that numerical modelling captures the effect of different boundary conditions in the calibration

chamber. This could potentially be a way to correct the calibration chamber's results for the boundary effect. In addition, the implemented BC5 in MARCC was validated by this numerical analysis. It is observed that—despite the simplicity of the MARCC—the measured cone resistance with simulated field boundary conditions is in good agreement with a more sophisticated calibration chamber in the literature and also matches well with the numerical CPT results in an infinite soil mass. This finding is of great importance, as it allows for the use of MARCC's output for engineering practice with more confidence.

ACKNOWLEDGMENT

The Authors would like to acknowledge the support of the project "Vibro Drucksondierungen", FKZ: 0325906 A by the Federal Ministry for Economic Affairs and Energy (BMWi) and the MARUM—Center for Marine Environmental Sciences, University of Bremen. The crucial help and assistance of the engineering and technician team of the geotechnical laboratory at MARUM, Marc Huhndorf, Joann Schmid, Wolfgang Schunn, and Tim Stanski are also greatly appreciated.

REFERENCES

Abaqus/Explicit User's Manual, Version 6.11 (2011) Dassault Syste`mes Simulia Corporation. Providence, Rhode Island, USA.

Butlanska, J., Arroyo, M. & Gens, A. 2009. Virtual calibration chamber CPT on Ticino sand. Second International Symposium on Cone Penetration Testing, CPT'10, At Humtington Beach, California, USA, Volume: 2.

DIN 18126 (1996) Bestimmung der Dichte nichtbindiger Böden den bei lockerster und dichtester Lagerung. Baugrund, Untersuchung von Bodenproben, vol DIN 18126:1996–11. Deutsches Institut für Normung, Berlin.

Fleischer, M., Kreiter, S., Mörz, T. & Hundorf, M. 2016. A Small Volume Calibration Chamber for Cone Penetration Testing (CPT) on Submarine Soils. Submarine Mass Movements and their Consequences, Advances in Natural and Technological Hazards Research 41.

Hu, Y., & Randolph, M.F. 1998. A practical numerical approach for large deformation problems in soil.. *Int. J. Numer. Anal. Meth. Geomech.,* 22: 327–350.

Huang, A.B. & Hsu, H.H. 2005. Cone penetration tests under simulated field conditions. *Geotechnique,* 55(5): 345–354.

Jamiolkowski, M., Presti, D.C.F. & Manassero, M., 2003. Evaluation of relative density and shear strength of sands from CPT and DMT. Symposium on Soil Behavior and Soft Ground Construction Honoring Charles C. "Chuck" Ladd.

Ladanyi, B. 1972. In Situ determination of undrained stress-strain behavior of sensitive clays with the pressuremeter. *Canadian Geotechnical Journal*, 9:313–319.

Mayne, P.W. & Kulhawy, F.H. 1991. Calibration chamber database and boundary effects correction for CPT data. Proceedings of the First International Symposium on Calibration Chamber Testing/ISOCCTl, Potsdam, New York.

Parkin, A.K. & Lunne, T. 1982. Boundary effects in the laboratory calibration of a cone penetrometer for sand. Proceeding of 2nd European symposium of penetration testing, Amsterdam, the Netherlands, 761–768.

Salgado, R. & Jamiolkowski, M. 2001. Calibration chamber size effects on penetration resistance in sand. *Journal of Geotechnical and Geoenvironmental Engineering*, 878–888.

Schnaid, F. & Houlsby, G.T. 1991. An assessment of chamber size effects in the calibration of in situ tests in sand. *Geotechnique,* 41(3): 437–445.

Susila, E. & Hryciw, R.D. 2003. Large displacement FEM modelling of the cone penetration test (CPT) in normally consolidated sand. *Int. J. Numer. Anal. Meth. Geomech.,* 27: 585–602.

Tolooiyan, A. & Gavin, K. 2011. Modelling the cone penetration test in sand using cavity expansion and arbitrary Lagrangian Eulerian finite element methods. *Computers and Geotechnics*, 38: 482–490.

Wichtmann, T. 2005. Explicit accumulation model for non-cohesive soils under cyclic loading, Inst. für Grundbau und Bodenmechanik Bochum University, Germany.